

# X-ray illumination of the ejecta of supernova 1987A

J. Larsson<sup>1</sup>, C. Fransson<sup>1</sup>, G. Östlin<sup>1</sup>, P. Gröningsson<sup>1</sup>, A. Jerkstrand<sup>1</sup>, C. Kozma<sup>1</sup>, J. Sollerman<sup>1</sup>, P. Challis<sup>2</sup>, R. P. Kirshner<sup>2</sup>, R. A. Chevalier<sup>3</sup>, K. Heng<sup>4</sup>, R. McCray<sup>5</sup>, N. B. Suntzeff<sup>6</sup>, P. Bouchet<sup>7</sup>, A. Crotts<sup>8</sup>, J. Danziger<sup>9</sup>, E. Dwek<sup>10</sup>, K. France<sup>11</sup>, P. M. Garnavich<sup>12</sup>, S. S. Lawrence<sup>13</sup>, B. Leibundgut<sup>14</sup>, P. Lundqvist<sup>1</sup>, N. Panagia<sup>15,16,17</sup>, C. S. J. Pun<sup>18</sup>, N. Smith<sup>19</sup>, G. Sonneborn<sup>10</sup>, L. Wang<sup>20</sup> & J. C. Wheeler<sup>21</sup>

**When a massive star explodes as a supernova, substantial amounts of radioactive elements—primarily <sup>56</sup>Ni, <sup>57</sup>Ni and <sup>44</sup>Ti—are produced<sup>1</sup>. After the initial flash of light from shock heating, the fading light emitted by the supernova is due to the decay of these elements<sup>2</sup>. However, after decades, the energy powering a supernova remnant comes from the shock interaction between the ejecta and the surrounding medium<sup>3</sup>. The transition to this phase has hitherto not been observed: supernovae occur too infrequently in the Milky Way to provide a young example, and extragalactic supernovae are generally too faint and too small. Here we report observations that show this transition in the supernova SN 1987A in the Large Magellanic Cloud. From 1994 to 2001, the ejecta faded owing to radioactive decay of <sup>44</sup>Ti as predicted. Then the flux started to increase, more than doubling by the end of 2009. We show that this increase is the result of heat deposited by X-rays produced as the ejecta interacts with the surrounding material. In time, the X-rays will penetrate farther into the ejecta, enabling us to analyse the structure and chemistry of the vanished star.**

Owing to the proximity of SN 1987A (located only 160,000 light yr away), we can study the evolution of the supernova in great detail. The central ejecta are surrounded by a ring of circumstellar material (Fig. 1) that was shed from the star 20,000 yr before the explosion in 1987<sup>4</sup>. Since the explosion, the ejecta have been expanding, and now the outer parts of the ejecta are colliding with the ring, causing it to brighten at all wavelengths<sup>5–8</sup>. The dense, central part of the ejecta contains most of the mass from the disrupted star and acts as a calorimeter for the energy input to the supernova. We have determined the energy input by tracking the energy output with the NASA Hubble Space Telescope (HST).

Because the ejecta are roughly elliptical in projection on the sky, we used an elliptical aperture to measure the brightness. To monitor a constant mass of expanding material, we allowed the measuring aperture to expand linearly with time. The axes of the aperture were therefore three times larger in 2009 than in 1994 (Fig. 1). Using this aperture, we determined the R- and B-band light curves of the ejecta, as shown in Fig. 2 (see Supplementary Table 1 and Supplementary Information, section 1, for further details of the observations and light curves). Our measurements show that the flux from the ejecta decays during the first ~5,000 d after the explosion, as expected from radioactive input, but then starts to increase, reaching a level that is two to three times higher at around day 8,000 (end of 2009). A new energy source must be present in addition to radioactive decay. Below, we consider a model for the declining phase and then discuss the new energy source that is responsible for the observed increase in flux.

The energy input to the declining phase of the light curve after ~1,500 d is expected to come from positrons produced in the decay of <sup>44</sup>Ti (refs 2, 9, 10). To test this, we use a model<sup>2</sup> with abundances taken from the 14E1 explosion model<sup>11</sup> and a <sup>44</sup>Ti mass of  $1.4 \times 10^{-4} M_{\odot}$  (ref. 12; Supplementary Information, section 3), where  $M_{\odot}$  is the solar mass. The model is shown in Fig. 3 together with the observed broadband luminosities. The good agreement with the observations up to day 5,000 confirms that the <sup>44</sup>Ti positrons provide the energy input up to this point. However, after day 5,000 the model fails to describe the light curve; radioactive decay cannot explain the increase in flux that we observe.

One possible origin for the flux increase is the reverse shock that results from the interaction between the ejecta and the H II region inside the ring<sup>13–16</sup>. The reverse shock produces strong Ly $\alpha$  and H $\alpha$  emission, which increased by a factor of ~1.7 between 2004 and 2010<sup>16</sup>. Although most of this emission originates close to the ring, there is also a component of projected high-velocity H $\alpha$  emission that can be traced to the central parts of the ejecta<sup>16</sup> and which would therefore contribute to the flux we measure. To determine the contribution of the reverse shock to our light curves, we have examined HST Space Telescope Imaging Spectrograph spectra from 2004 and 2010 (Supplementary Information, section 2, and Supplementary Fig. 5). The reverse shock can be isolated in the spectra because of its boxy line profile, allowing us to place a limit on its contribution at  $\lesssim 20\%$ . Furthermore, this changes only marginally between 2004 and 2010, as the expanding measuring aperture remains well inside the area where most of the shock emission is seen. Importantly, an increase in flux is also seen in the [Ca II] doublet lines at rest wavelengths 7,292 Å and 7,324 Å between 2000 and 2010 (determined from Ultraviolet and Visual Echelle Spectrograph observations at the Very Large Telescope; Fig. 2). These lines have speeds of  $\lesssim 5,000 \text{ km s}^{-1}$ , implying that they originate in the inner ejecta (the projected ejecta speed near the edge of the ring is  $\gtrsim 7,000 \text{ km s}^{-1}$  at the present time). We conclude that the increase in flux occurs primarily in the inner ejecta and cannot be explained by emission from the shock region.

We believe that the strong X-ray flux produced in the ring collision is the dominant source of energy input to the ejecta. The X-ray flux from the ring increased by a factor of ~3 in the 0.5–10-keV band between day 6,000 and day 8,000<sup>6</sup>, similar to what we find for the optical emission from the ejecta. To investigate this, we calculated the fraction of X-rays absorbed by the ejecta from a point source located at the ring, using the partially mixed 14E1 explosion model<sup>17</sup>. As shown in Supplementary Fig. 6, most of the observed X-ray flux is

<sup>1</sup>Department of Astronomy, The Oskar Klein Centre, Stockholm University, 106 91 Stockholm, Sweden. <sup>2</sup>Harvard-Smithsonian Center for Astrophysics, 60 Garden Street, MS-19, Cambridge, Massachusetts 02138, USA. <sup>3</sup>Department of Astronomy, University of Virginia, Charlottesville, Virginia 22903, USA. <sup>4</sup>Eidgenössische Technische Hochschule Zürich, Institute for Astronomy, Wolfgang-Pauli-Strasse 27, CH-8093 Zürich, Switzerland. <sup>5</sup>JILA, University of Colorado, Boulder, Colorado 803090-0440, USA. <sup>6</sup>George P. and Cynthia Woods Mitchell Institute for Fundamental Physics and Astronomy, Texas A&M University, Department of Physics and Astronomy, College Station, Texas 77843, USA. <sup>7</sup>DSM/IRFU/Service d'Astrophysique Commissariat à l'Energie Atomique et aux Energies Alternatives, Saclay, Orme des Merisiers, FR 91191 Gif-sur-Yvette, France. <sup>8</sup>Department of Astronomy, Mail Code 5240, Columbia University, 550 West 120th Street, New York, New York 10027, USA. <sup>9</sup>Osservatorio Astronomico di Trieste, Via Tiepolo 11, Trieste 34131, Italy. <sup>10</sup>NASA Goddard Space Flight Center, Code 665, Greenbelt, Maryland 20771, USA. <sup>11</sup>Center for Astrophysics and Space Astronomy, University of Colorado, Boulder, Colorado 80309, USA. <sup>12</sup>225 Nieuwland Science, University of Notre Dame, Notre Dame, Indiana 46556-5670, USA. <sup>13</sup>Department of Physics and Astronomy, Hofstra University, Hempstead, New York 11549, USA. <sup>14</sup>ESO, Karl-Schwarzschild-Strasse 2, 85748 Garching, Germany. <sup>15</sup>Space Telescope Science Institute, 3700 San Martin Drive, Baltimore, Maryland 21218, USA. <sup>16</sup>INAF-CT, Osservatorio Astrofisico di Catania, Via S. Sofia 78, I-95123 Catania, Italy. <sup>17</sup>Supernova Limited, OYV #131, Northsound Road, Virgin Gorda, British Virgin Islands. <sup>18</sup>Department of Physics, University of Hong Kong, Pok Fu Lam Road, Hong Kong, China. <sup>19</sup>Steward Observatory, University of Arizona, 933 North Cherry Avenue, Tucson, Arizona 85721, USA. <sup>20</sup>Department of Physics and Astronomy, Texas A&M University, College Station, Texas 77843-4242, USA. <sup>21</sup>Department of Astronomy, University of Texas, Austin, Texas 78712-0259, USA.

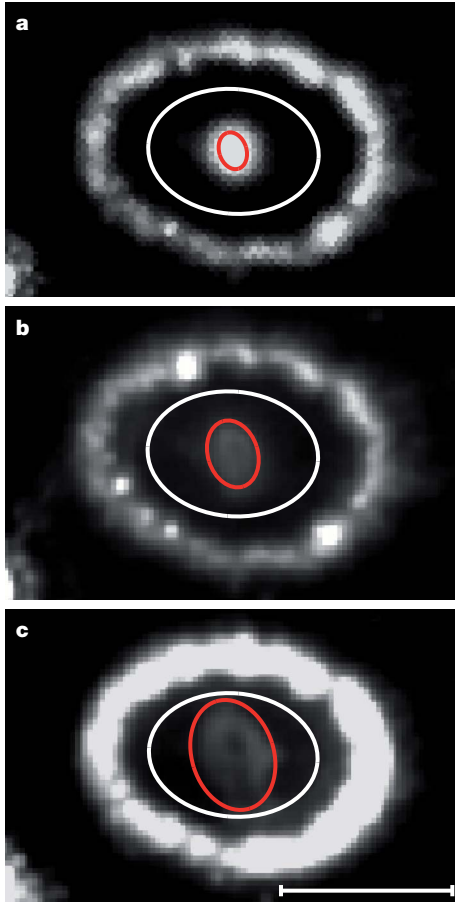


**Figure 1 | HST R-band images.** The observing dates are 1994 September 24 (a), 2000 November 13 (b) and 2009 April 29 (c), which correspond to 2,770, 5,012 and 8,101 d after the explosion, respectively. The scale bar in c represents  $1''$ . The circumstellar ring is inclined at an angle of  $45^\circ$  with respect to the line of sight and is approximately 1.3 light yr across. The red ellipse shows the expanding aperture used for the light curve in Fig. 2. By using an initial semi-major axis of  $0.11''$  for the observation in 1994, we always follow the bright, central part of the ejecta without being significantly affected by emission from the circumstellar ring. The white ellipse shows the fixed aperture used for one of the light curves in Supplementary Fig. 2. The R-band emission from the ejecta is dominated by H $\alpha$  emission with a small contribution from [Ca I] and [Ca II] lines, whereas the B band (Supplementary Fig. 1) is dominated by H I, Fe I and Fe II lines<sup>12,22</sup>. Only the densest, central parts of the ejecta are visible, owing to the low surface brightness of the outer parts. In reality, the ejecta extend to the ring, as is evident from the strong interaction with the ring.

absorbed in the core region of the ejecta (corresponding to speeds less than  $5,000 \text{ km s}^{-1}$ ), where most of the heavy elements reside. At an energy of  $\sim 0.35 \text{ keV}$ , which corresponds to the temperature of the dominant component in the X-ray spectrum<sup>18</sup>, the fraction of flux absorbed by the ejecta at  $t_{\text{yr}}$  years can be approximated by  $1.6 \times 10^{-3} t_{\text{yr}}^{1.67}$  (the increase with time is mainly due to the increasing solid angle of the expanding ejecta, assumed to be spherical, as seen from the ring). This gives a present-day absorbed X-ray luminosity of  $\sim 5.0 \times 10^{35} \text{ erg s}^{-1}$ . In this calculation, we have neglected the weaker, highest-energy component that contributes to the X-ray spectrum<sup>18</sup>. We note that this does not significantly affect the estimate of the absorbed flux, although the hard X-rays may be important owing to their greater penetrating power.

To model the ejecta light curve produced by input from the X-rays, we scaled the observed X-ray flux<sup>6</sup> by the fraction absorbed at  $0.35 \text{ keV}$ , multiplied the resulting flux by a constant (corresponding to the conversion efficiency from X-rays to optical emission) and added this to the radioactive energy input. Figure 3 shows the scaled X-ray flux together with the observed light curves. This model follows the general

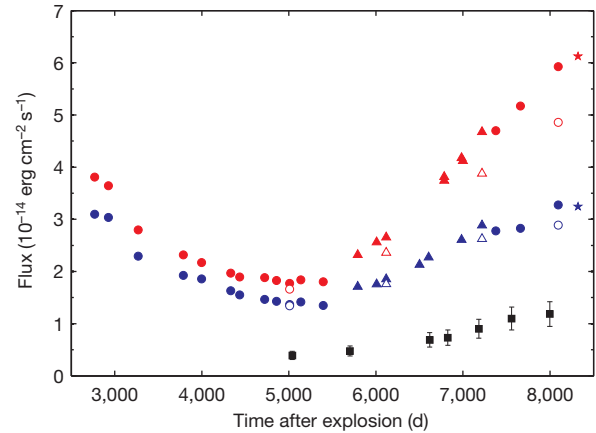


**Figure 2 | Light curves of the ejecta in different wavebands.** Data points from the HST Wide Field and Planetary Camera 2 (WFPC2), Advanced Camera for Surveys (ACS) and Wide Field and Camera 3 (WFC3) are shown as dots, triangles and stars, respectively. Red and blue symbols correspond to the R and B bands, respectively. A correction factor has been applied to the ACS and WFC3 fluxes to account for the differences between these instruments and WFPC2. To quantify the contamination from the brightening circumstellar ring, we created detailed models of the ring for a number of different epochs (Supplementary Information, section 1, and Supplementary Figs 3 and 4). The open symbols show the ejecta fluxes after the contribution from the ring has been removed. Although the contamination from the ring increases with time, it never exceeds  $\sim 20\%$  of the flux from the ejecta. The statistical errors in the HST fluxes are smaller than the data points, and systematic errors are discussed in the Supplementary Information, section 1. The black squares show the flux of the [Ca II] doublet lines at rest wavelengths  $7,291.5 \text{ \AA}$  and  $7,323.9 \text{ \AA}$ , measured using the Ultraviolet and Visual Echelle Spectrograph of the Very Large Telescope at the European Southern Observatory (error bars, s.d.). These lines are free from contamination from the circumstellar ring and the reverse shock. We note the decreasing flux during the first  $\sim 5,000 \text{ d}$  and the increase thereafter, indicating an extra source of energy. A further indication that the energy source has changed is that the colour, determined from the flux ratio between the B and R bands, changes from a level of  $\sim 0.8$  up to day 5,000 to a value close to  $\sim 0.6$  on day 8,000.

trend of the observed fluxes in both bands, although we note that a more accurate model would need to take into account the detailed shape of the X-ray spectrum and the reprocessing of the X-rays into optical emission. The required conversion efficiency from X-rays to optical emission in our model is 5.0% in the R band and 3.1% in the B band.

The conversion of X-rays to optical/infrared emission is similar to that of the  $^{44}\text{Ti}$  positrons. Both involve degradation of non-thermal electrons into heating, ionization and excitation. For a typical ionization fraction of  $10^{-3}$ – $10^{-2}$ , the expected efficiency of conversion from X-rays to H $\alpha$  emission (the dominant line in the R band) is  $\sim 5\%$  (Supplementary Information, section 3). This conversion factor is consistent with the scaling factor we used to model the light curve. Similar arguments apply to the B band. Furthermore, the density in the core is high enough for the timescale of recombination to be shorter than the expansion timescale, ensuring a balance between the energy input and output.

Other possible explanations for the increase in flux include input from a central pulsar<sup>19</sup>, a transition from optically thick to optically thin dust and positron leakage from the iron-rich regions. We find that input from a pulsar is unlikely for several reasons. In particular, it would be a strange coincidence for the emission from the pulsar to mimic the increasing X-ray flux from the ring interaction. Also, we expect the energy input from a pulsar to be concentrated towards the low-velocity material at the centre of the ejecta, but observations of the H $\alpha$  and [Ca II] lines show that the increase occurs for speeds up to  $\sim 5,000 \text{ km s}^{-1}$ . We also note that constraints on a point source at the centre of SN 1987A have already been obtained using HST data

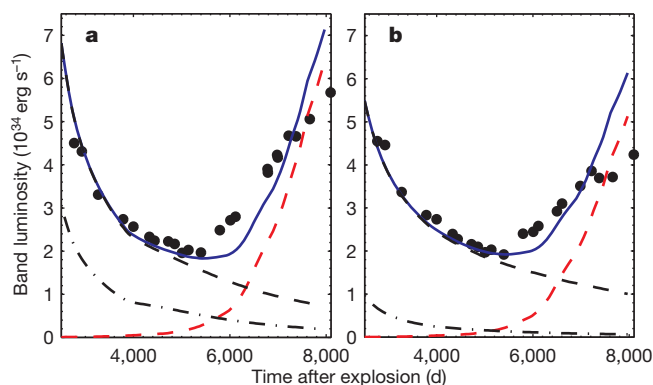


**Figure 3 | Evolution of the luminosity from the ejecta in the R and B bands.** **a**, R band; **b**, B band. The black dashed lines show a model with only radioactive input, mainly from  $^{44}\text{Ti}$ . The  $^{44}\text{Ti}$  mass used for the model is  $1.4 \times 10^{-4} M_{\odot}$  (ref. 12), as determined from a detailed analysis that takes into account the effects of scattering and fluorescence of the ultraviolet flux, as well as a correction for internal dust<sup>23,24</sup> (here taken to have a 50% covering factor of the core inside the radius where the ejecta speed is  $2,000 \text{ km s}^{-1}$ ). The dot-dash lines show the light curves with no  $^{44}\text{Ti}$ , illustrating the necessity of including this isotope. The red dashed lines show a model based on a constant fraction of the observed X-ray flux<sup>6</sup>, corrected for the fraction of flux absorbed by the ejecta (Supplementary Fig. 7). The blue solid line shows the sum of both models (black and red dashed). The R and B bands contain 5% and 3% of the total bolometric flux, respectively, and we expect these fractions to remain roughly constant in time. This is because the relative amount of energy resulting in heating, ionization and excitation will remain nearly constant as long as the ionization by the X-rays is  $\lesssim 10^{-2}$ . It is clear from this figure that there is a transition at  $\sim 5,000 \text{ d}$  from a radioactivity-dominated phase to a phase dominated by the X-ray input from the collision with the ring.

taken near the minimum of the ejecta light curve<sup>20</sup>. A change in the properties of the dust or a transition in the positron deposition process is also unable to explain the observed increase in flux quantitatively (Supplementary Information, section 4).

We conclude that SN 1987A has made a transition from a radioactively dominated phase to a phase dominated by the X-ray input from the ring collision. This conclusion has interesting implications for the observed morphology. In particular, most of the X-rays are likely to be absorbed at the boundary of the ejecta core, where the density increases rapidly. This may lead to the light from the ejecta being emitted in a ring that is concentrated in the plane of the circumstellar ring. The ‘hole’ in the ejecta (Fig. 1), which has become more pronounced since about 2001, may in fact be a result of this rather than reflecting the true density distribution or dust obscuration. The asymmetric morphology seen at speeds of  $\lesssim 3,000 \text{ km s}^{-1}$  in the near-infrared [Si I] and [Fe II] lines<sup>21</sup> is, however, likely to be intrinsic to the metal core. By studying future changes in the morphology of the ejecta, we will be able to understand the origin of this asymmetry.

In the future, the density of the ejecta will decrease and the fraction of X-rays absorbed will grow (Supplementary Fig. 7). As a result, the ionization will increase and a smaller fraction of the X-ray flux will produce line excitation. A larger fraction will go into heating, leading to an increase in the mid-infrared flux and a flattening of the optical light curves. In time, the X-rays will also penetrate deeper layers of the ejecta, thereby allowing us to probe the chemical structure of the innermost ejecta. This will be a novel form of X-ray tomography.

Received 31 January; accepted 31 March 2011.

Published online 8 June 2011.

1. Woosley, S. E., Heger, A. & Weaver, T. A. The evolution and explosion of massive stars. *Rev. Mod. Phys.* **74**, 1015–1071 (2002).
2. Fransson, C. & Kozma, C. Radioactivities and nucleosynthesis in SN 1987A. *N. Astron. Rev.* **46**, 487–492 (2002).
3. McKee, C. F. in *Young Supernova Remnants* (eds Holt, S. S. & Hwang, U.) 17–28 (Am. Inst. Phys. Conf. Proc. 565, Springer, 2001).
4. Morris, T. & Podsiadlowski, P. The triple-ring nebula around SN 1987A: fingerprint of a binary merger. *Science* **315**, 1103–1105 (2007).
5. Gröningsson, P. *et al.* Time evolution of the line emission from the inner circumstellar ring of SN 1987A and its hot spots. *Astron. Astrophys.* **492**, 481–491 (2008).
6. Racusin, J. L. *et al.* X-ray evolution of SNR 1987A: the radial expansion. *Astrophys. J.* **703**, 1752–1759 (2009).
7. Zanardo, G. *et al.* Multifrequency radio measurements of supernova 1987A over 22 years. *Astrophys. J.* **710**, 1515–1529 (2010).
8. Dwek, E. *et al.* Five years of mid-infrared evolution of the remnant of SN 1987A: the encounter between the blast wave and the dusty equatorial ring. *Astrophys. J.* **722**, 425–434 (2010).
9. Timmes, F. X., Woosley, S. E., Hartmann, D. H. & Hoffman, R. D. The production of  $^{44}\text{Ti}$  and  $^{60}\text{Co}$  in supernovae. *Astrophys. J.* **464**, 332–341 (1996).
10. Diehl, R. & Timmes, F. X. Gamma-ray line emission from radioactive isotopes in stars and galaxies. *Publ. Astron. Soc. Pacif.* **110**, 637–659 (1998).
11. Shigeyama, T. & Nomoto, K. Theoretical light curve of SN 1987A and mixing of hydrogen and nickel in the ejecta. *Astrophys. J.* **360**, 242–256 (1990).
12. Jerkstrand, A., Fransson, C. & Kozma, C. The  $^{44}\text{Ti}$ -powered spectrum of SN 1987A. *Astron. Astrophys.* (in the press); preprint at (<http://arxiv.org/abs/1103.3653>) (2011).
13. Michael, E. *et al.* Hubble Space Telescope observations of high-velocity Ly $\alpha$  and H $\alpha$  emission from supernova remnant 1987A: the structure and development of the reverse shock. *Astrophys. J.* **593**, 809–830 (2003).
14. Smith, N. *et al.* The reverse shock of SNR 1987A at 18 years after outburst. *Astrophys. J.* **635**, L41–L44 (2005).
15. Heng, K. *et al.* Evolution of the reverse shock emission from SNR 1987A. *Astrophys. J.* **644**, 959–970 (2006).
16. France, K. *et al.* Observing supernova 1987A with the refurbished Hubble Space Telescope. *Science* **329**, 1624–1627 (2010).
17. Blinnikov, S., Lundqvist, P., Bartunov, O., Nomoto, K. & Iwamoto, K. Radiation hydrodynamics of SN 1987A. I. Global analysis of the light curve for the first 4 months. *Astrophys. J.* **532**, 1132–1149 (2000).
18. Zhekov, S. A., Park, S., McCray, R., Racusin, J. L. & Burrows, D. N. Evolution of the Chandra CCD spectra of SNR 1987A: probing the reflected-shock picture. *Mon. Not. R. Astron. Soc.* **721**, 518–529 (2010).
19. Woosley, S. E., Hartmann, D. & Pinto, P. A. Hard emission at late times from SN 1987A. *Astrophys. J.* **346**, 395–404 (1989).
20. Graves, G. J. M. *et al.* Limits from the Hubble Space Telescope on a point source in SN 1987A. *Astrophys. J.* **629**, 944–959 (2005).
21. Kjaer, K., Leibundgut, B., Fransson, C., Jerkstrand, A. & Spyromilio, J. The 3-D structure of SN 1987A’s inner ejecta. *Astron. Astrophys.* **517**, A51–A60 (2010).
22. Chugai, N. N., Chevalier, R. A., Kirshner, R. P. & Challis, P. M. Hubble Space Telescope spectrum of SN 1987A at an age of 8 years: radioactive luminescence of cool gas. *Astrophys. J.* **483**, 925–940 (1997).
23. Lucy, L. B., Danziger, I. J., Gouiffes, C. & Bouchet, P. in *Supernovae* (ed. Woosley, S. E.) 82–94 (Springer, 1991).
24. Wooden, D. H. *et al.* Airborne spectrophotometry of SN 1987A from 1.7 to 12.6 microns: time history of the dust continuum and line emission. *Astrophys. J.* **88** (suppl.), 477–507 (1993).

**Supplementary Information** is linked to the online version of the paper at [www.nature.com/nature](http://www.nature.com/nature).

**Acknowledgements** This work was supported by the Swedish Research Council and the Swedish National Space Board. Support for the HST observing programme was provided by NASA through a grant from the Space Telescope Science Institute, which is operated by the Association of Universities for Research in Astronomy, Inc.

**Author Contributions** J.L. carried out the data reduction and analysis together with G.Ö., P.G., B.L., J.S. and P.C.; C.F. performed the theoretical modelling together with A.J. and C.K.; and J.L. and C.F. wrote the paper. R.P.K. is the principal investigator for the HST/SAINTS collaboration. All authors discussed the results and commented on the manuscript.

**Author Information** Reprints and permissions information is available at [www.nature.com/reprints](http://www.nature.com/reprints). The authors declare no competing financial interests. Readers are welcome to comment on the online version of this article at [www.nature.com/nature](http://www.nature.com/nature). Correspondence and requests for materials should be addressed to J.L. ([josefin.larsson@astro.su.se](mailto:josefin.larsson@astro.su.se)) or C.F. ([claes@astro.su.se](mailto:claes@astro.su.se)).